

# Iodometry-Assisted Liquid Chromatography Electrospray Ionization Mass Spectrometry for Analysis of Organic Peroxides: An Application to Atmospheric Secondary Organic Aerosol

Ran Zhao,<sup>\*,†,‡</sup> Christopher M. Kenseth,<sup>†,‡</sup> Yuanlong Huang,<sup>‡</sup> Nathan F. Dalleska,<sup>§</sup> and John H. Seinfeld<sup>†,||</sup>

<sup>†</sup>Division of Chemistry and Chemical Engineering, California Institute of Technology, Pasadena, California 91125, United States

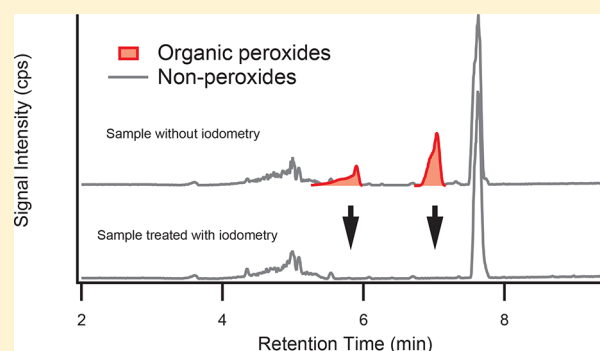
<sup>‡</sup>Division of Geological and Planetary Sciences, California Institute of Technology, Pasadena, California 91125, United States

<sup>§</sup>Environmental Analysis Center, California Institute of Technology, Pasadena, California 91125, United States

<sup>||</sup>Division of Engineering and Applied Science, California Institute of Technology, Pasadena, California 91125, United States

## Supporting Information

**ABSTRACT:** Organic peroxides comprise a significant fraction of atmospheric secondary organic aerosol (SOA). Detection and quantification of particle-phase organic peroxides are highly challenging, and current efforts rely significantly on filter extraction and offline mass spectrometry (MS). Here, a novel technique, iodometry-assisted liquid chromatography electrospray ionization mass spectrometry (iodometry-assisted LC-ESI-MS), is developed and evaluated with a class of atmospherically relevant organic peroxides,  $\alpha$ -acyloxyalkyl hydroperoxides, synthesized via liquid ozonolysis. Iodometry-assisted LC-ESI-MS unambiguously distinguishes organic peroxides, compensating for the lack of functional group information that can be obtained with MS. This technique can be versatile for a wide spectrum of environmental analytical applications for which a molecular-level identification of organic peroxide is required. Here, iodometry-assisted LC-ESI-MS is applied to the water-soluble organic carbon (WSOC) of  $\alpha$ -pinene SOA. Unexpectedly, a limited number of detectable compounds in WSOC appear to be organic peroxides, despite the fact that spectroscopy-based iodometry indicates 15% of WSOC mass is associated with organic peroxides. This observation would be consistent with decomposition of multifunctional organic peroxides to small peroxides that can be quantified by spectroscopy-based iodometry but not by LC-ESI-MS. Overall, this study raises concerns regarding filter extraction-based studies, showing that assignment of organic peroxides solely on the basis of MS signatures can be misleading.



## INTRODUCTION

Organic peroxides are ubiquitous in the atmospheric environment, participating in the oxidation of  $\text{SO}_2$  to form acid rain,<sup>1</sup> serving as a reservoir for atmospheric oxidants,<sup>2</sup> and potentially contributing to the adverse health effects of air pollution.<sup>3</sup> Recent studies have revealed a critical role that organic peroxides play in the formation of secondary organic aerosol (SOA), submicrometer particulate matter that forms in the atmosphere via condensation of oxidation products of volatile organic compounds (VOCs).<sup>4</sup> Despite the prominent role that SOA plays in air quality and the global climate, our understanding of the reaction mechanisms and products of VOC oxidation remains incomplete. In particular, the identity and chemistry of organic peroxides represent important missing aspects.

On a global scale, biogenic monoterpenes ( $\text{C}_{10}\text{H}_{16}$ ) are important precursors to SOA. Estimated global SOA production from mono- and sesquiterpenes varies from 14 to

246 Tg/year.<sup>5,6</sup>  $\alpha$ -Pinene is the dominant monoterpene by mass<sup>7</sup> and is readily oxidized in the atmosphere by the major oxidants,  $\text{O}_3$  and the OH radical. It has been established that SOA arising from  $\alpha$ -pinene contains a substantial amount of total organic peroxides.<sup>8,9</sup> Quantification of organic peroxides in SOA extracts has been successful using spectroscopic techniques, such as iodometry.<sup>8,10–12</sup> Iodometry proceeds as  $\text{R}_1\text{OOR}_2 + 2\text{I}^- + 2\text{H}^+ \rightarrow \text{R}_1\text{OH} + \text{R}_2\text{OH} + \text{I}_2$ , followed by  $\text{I}_2 + \text{I}^- \rightarrow \text{I}_3^-$ ,<sup>13</sup> where  $\text{R}_1$  and  $\text{R}_2$  represent any alkyl group or H. With acid catalysis,  $\text{I}^-$  reduces an organic peroxide molecule to the corresponding alcohols, liberating  $\text{I}_2$  that subsequently forms  $\text{I}_3^-$  in an excess of  $\text{I}^-$ . The characteristic absorption of  $\text{I}_3^-$  reaches a peak at 350 nm and can be measured by ultraviolet–

Received: September 20, 2017

Revised: January 10, 2018

Accepted: January 25, 2018

Published: January 25, 2018

visible (UV-vis) spectrometry. As  $I^-$  reacts with essentially all types of organic peroxides,<sup>14</sup> iodometry determines the total organic peroxide content. Molecular-level identification of particle-phase organic peroxides is more challenging, because of the chemical complexity of SOA components, a lack of authentic organic peroxide chemical standards, and their chemical instability. A number of recent studies have reported decomposition of SOA organic peroxides in the particle phase<sup>12,15</sup> and the aqueous phase.<sup>16</sup>

Recent application of liquid chromatography electrospray ionization mass spectrometry (LC-ESI-MS) to extracted SOA components has significantly advanced our understanding of particle-phase organic compounds, including both monomers and dimers,<sup>17–29</sup> a number of which have been proposed to be organic peroxides. In particular, it is proposed that the stabilized Criegee intermediate (SCI) formed during ozonolysis can react with organic acids and form a class of hydroperoxy dimer esters,  $\alpha$ -acyloxyalkyl hydroperoxides ( $\alpha$ AAHPs).<sup>15,17,18,30,31</sup> The importance of  $\alpha$ AAHPs in the ambient atmosphere remains unclear, but a  $\leq 16\%$  contribution by mass to laboratory-generated SOA has been reported.<sup>17</sup> Additionally, gas-phase measurements using chemical ionization mass spectrometry have detected highly oxidized multifunctional organic compounds (HOMs), which bear multiple hydroperoxy functional groups and arise from repeated intramolecular hydrogen-abstraction reactions.<sup>32,33</sup> HOMs exhibit extremely low volatility, and their presence in the particle phase has been reported.<sup>34–37</sup> These studies have highlighted novel SOA formation pathways in which organic peroxides play a pivotal role. Determination of such organic peroxides at the molecular level is critical and is the only means of revealing the underlying mechanisms of formation of SOA.

Although ESI-MS is a versatile technique for a wide spectrum of organic compounds,<sup>38,39</sup> unambiguous identification of organic peroxides using MS-based techniques is challenging, given that MS provides limited information about functional groups. A number of studies have used ESI-MS to detect synthesized organic peroxides, including peracids,<sup>40,41</sup> alkylhydroperoxides,<sup>42</sup> peroxy esters,<sup>29</sup> diacyl peroxides,<sup>43</sup> and  $\alpha$ AAHPs.<sup>44</sup> Despite the capability of ESI-MS for organic peroxide detection, detection of organic peroxide is highly sensitive to specific conditions employed in each ESI-MS instrument.

The primary objective of this study is to develop and demonstrate the applicability of a novel technique, iodometry-assisted LC-ESI-MS, to unambiguously distinguish organic peroxides present in a complex chemical matrix. The method is evaluated with  $\alpha$ AAHPs synthesized via liquid-phase ozonolysis. For the first time, iodometry is employed not only to determine the total peroxide content but also to provide molecularly resolved information by coupling to LC-ESI-MS. We have applied iodometry-assisted LC-ESI-MS to investigate organic peroxides present in the water-soluble fraction of  $\alpha$ -pinene SOA. Measurements of water-soluble organic carbon (WSOC) in SOA can be performed using filter extraction and/or the particle-into-liquid sampler (PILS).<sup>45</sup> WSOC has gained attention as a proxy for the oxygenated fraction of SOA<sup>46</sup> that can dissolve in cloudwater and undergo multiphase chemistry.<sup>47–49</sup>

## ■ EXPERIMENTAL SECTION

**Chemicals.** All chemicals were used without further purification. The following chemicals were purchased from

Sigma-Aldrich: adipic acid (99%),  $\alpha$ -pinene (>99%), benzoylperoxide (Luperox, 75%), *cis*-pinonic acid (98%), D-sorbitol (>98%), hydrogen peroxide ( $H_2O_2$ , 50% in water), lauroyl peroxide (Luperox, 97%), leucine enkephalin [ $>95\%$ , high-performance liquid chromatography (HPLC) grade], meso-erythritol (>99%), pinic acid (custom-synthesized), potassium hydrogen phthalate (>99.95%), potassium iodide (KI, 99%), and *tert*-butyl hydroperoxide (Luperox, 50% in water). Chemicals were also purchased from other sources: acetonitrile (EMD), ammonium sulfate [ $(NH_4)_2SO_4$ , Mallinckrodt Chemicals], formic acid (Fluka, HPLC grade, 50% in water), glacial acetic acid (Macron Fine Chemicals), and methylhydroperoxide (synthesized).

**SOA Generation and Collection.** SOA was generated in the steady state Caltech photooxidation flow tube (CPOT) reactor,<sup>50</sup> details of which are given in [section S1 of the Supporting Information](#). Briefly,  $\alpha$ -pinene (175 ppb) and  $O_3$  (1 ppm) reacted in the CPOT to generate SOA at room temperature without light or nitrogen oxides. No OH scavenger was added; therefore,  $\alpha$ -pinene is oxidized primarily by  $O_3$  with a contribution from the OH radical generated during ozonolysis. The total rate of gas flow through the CPOT was 12.5 L/min, giving rise to an average residence time of 3.5 min. Polydisperse  $(NH_4)_2SO_4$  seed aerosol was generated by aerosolizing an aqueous solution (0.01 M) with a custom-built atomizer, followed by using a diffuser dryer and a neutralizer. The relative humidity (RH) in the CPOT was approximately 10%.

Approximately 10 L/min of flow from the CPOT was introduced through a Teflon filter (Pall Life Sciences, 47 mm diameter and 2  $\mu$ m pore size) to collect SOA samples. A diffuser packed with activated charcoal was employed before the filter to remove  $O_3$  and gas-phase species to prevent continuous on-filter reactions and further partitioning of gas-phase species to the collected particles. One filter sample was collected per experiment, with collection times of 15–18 h. The mass of collected particle samples was typically 1–2 mg. Filters were frozen at  $-16^\circ C$  immediately after collection. Note that we employed collection times longer than those in previous studies (0.6–4 h)<sup>8,11,51,52</sup> to overcome the detection limits of offline analyses and to maximize detection of compounds by LC-ESI-MS.

**Synthesis of  $\alpha$ -Acyloxyalkyl Hydroperoxides ( $\alpha$ AAHPs).** Two  $\alpha$ AAHP species were synthesized as surrogates for multifunctional organic peroxides.<sup>17,30,31</sup> They were synthesized via liquid-phase ozonolysis with a method modified from a previous study.<sup>44</sup> Briefly,  $\alpha$ -pinene (50 mM) and an organic acid (10 mM) were dissolved in acetonitrile. A 5 mL aliquot of this solution was bubbled with an air stream containing roughly 100 ppm of  $O_3$  at a flow rate of 120 sccm for 5 min. The ozonolysis solution was immersed in an ice bath throughout the synthesis and storage to minimize decomposition.

The proposed pathway for formation of  $\alpha$ AAHPs, as well as their structures, is shown in [Figure 1](#). Briefly,  $\alpha$ -pinene reacts with  $O_3$  to form a primary ozonide that decomposes to form two possible Criegee intermediates. Upon interaction with the surrounding solvent molecules, stabilized Criegee intermediates (SCIs) are formed. The SCI reacts with the excess of the organic acid added to the solution, forming an  $\alpha$ AAHP species with two possible structural isomers. Two organic acids, pinonic acid and adipic acid, were chosen in this work to synthesize two different  $\alpha$ AAHPs. Pinonic acid was selected for

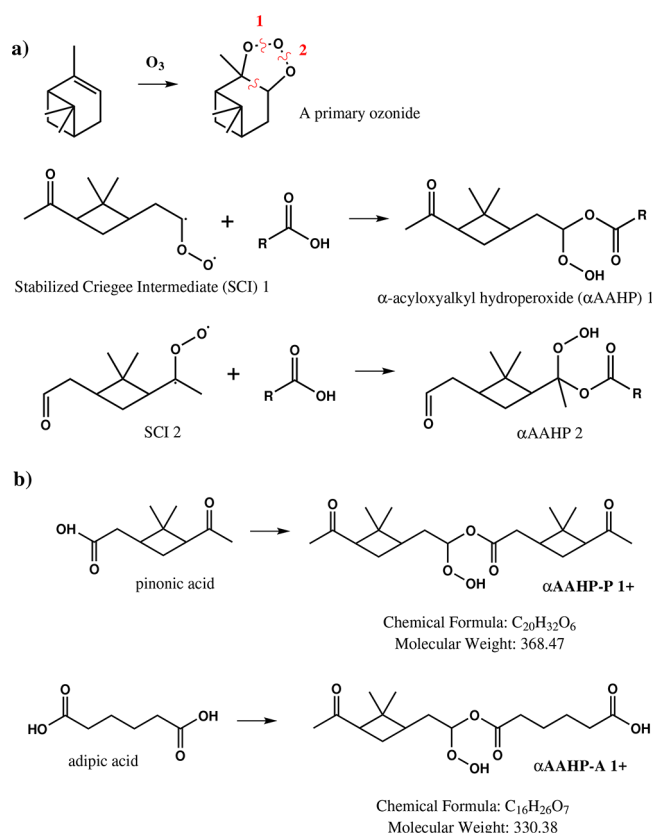


**Figure 1.** Schematic of the mechanism underlying the synthesis of the  $\alpha$ AAHP species. Reactions in panel (a) illustrate the general reaction between a stabilized Criegee intermediate (SCI) and an organic acid, giving rise to  $\alpha$ AAHP with two possible structural isomers. Reactions in panel (b) show the specific cases employed in this work to synthesize  $\alpha$ AAHP-P and  $\alpha$ AAHP-A. Only one structural isomer is shown for each of them.

its relevance in  $\alpha$ -pinene oxidation. Adipic acid, being a diacid, contains an additional carboxylic acid functional group for which  $\alpha$ AAHP-A is more easily detected by ESI<sup>−</sup>-MS. These two species are hereafter termed  $\alpha$ AAHP-P and  $\alpha$ AAHP-A, respectively.

**Offline Chemical Analyses.** The frozen filter samples were thawed and extracted in 10 mL of Milli-Q water (18.2 m $\Omega$ ) by being mechanically shaken before in-depth chemical analyses were performed. Sonication was avoided to prevent potential artifacts.<sup>10</sup>

**Total Organic Carbon (TOC).** The total organic carbon (TOC) content of the SOA extracts was quantified using a TOC analyzer (OI Analytical model 1030W). The total carbon (TC) method was employed, wherein all the carbon-containing species (i.e., both organic and inorganic) are oxidized to  $CO_2$  by sodium persulfate with phosphoric acid at 100 °C, with the  $CO_2$  detected by nondispersive infrared detection. The TC content measured in a blank filter extract was subtracted as the background. The limit of detection is 0.6 ppm of C, determined as  $3\sigma$  + the mean of the filter blank. The method was calibrated using potassium hydrogen phthalate, and the accuracy of the method was 5%, tested by measuring *meso*-erythritol and D-sorbitol solutions at known concentrations.

**Iodometry.** Formic acid or acetic acid was added to an aliquot of a WSOC sample to adjust the solution pH to 2 or 3, respectively. To this solution was added a concentrated potassium iodide (KI) aqueous solution, made fresh daily and

purged with  $N_2$  gas, such that the concentration of  $I^-$  in the solution was 60 mM. Immediately after the addition of KI, the solution was gently purged with  $N_2$  and placed in an airtight vial in the dark for 1 h before the UV–vis measurement was conducted with a spectrophotometer (Shimadzu, UV-1601). The method was calibrated prior to each experiment against a set of  $H_2O_2$  solutions, standardized with the molar absorptivity of  $H_2O_2$  at 254 nm. The calibration accounts for the reaction of  $I^-$  with dissolved  $O_2$  and confirms the linearity of the method. The detection limit of the current method is 1.5  $\mu$ M  $H_2O_2$  equivalent, determined as  $3\sigma$  of the water blank.

**Iodometry-Assisted LC-ESI-MS.** The instrument and methods employed for the LC-ESI-MS analysis have been described previously.<sup>22,23</sup> Briefly, the instrument consists of a Waters ACQUITY UPLC I-Class system, coupled to a quadrupole time-of-flight mass spectrometer (Xevo G2-S QToF). LC separation was performed on an ACQUITY BEH  $C_{18}$  column (2.1 mm  $\times$  50 mm) held at 30 °C. The total flow rate was 0.3 mL min<sup>−1</sup>, and the injection volume was 10  $\mu$ L. LC uses two eluents: A [0.1% (v/v) formic acid in water] and B (100% acetonitrile). The gradient was programmed as follows: 100% A from 0 to 2.0 min, 10% A and 90% B from 2.0 to 10.2 min, and 100% A from 10.2 to 12 min. ESI settings were as follows: capillary voltage, 2.0 kV; sampling cone voltage, 40 V; source offset, 80 V; source temperature, 120 °C; desolvation temperature, 400 °C; cone gas, 30 L h<sup>−1</sup>; desolvation gas, 650 L h<sup>−1</sup>. Leucine enkephalin was employed as the lock mass for accurate mass determination. The method stability is within 5%, as determined by frequent consistency tests. The positive (LC-ESI<sup>+</sup>-MS) and negative (LC-ESI<sup>−</sup>-MS) modes were used under the same settings, and data were acquired and processed with MassLynx version 4.1.

For a number of samples, the iodometry method described above was applied prior to the LC-ESI-MS measurement. Formic acid was used to adjust the solution pH to 2. To ensure the completion of iodometry, the iodometry solutions were allowed to react for 5–7 h before the LC-ESI-MS measurement was conducted. As iodometry selectively reacts away organic peroxides, it is hypothesized that organic peroxide compounds can be elucidated by a comparison of iodometry-treated samples and nontreated samples. Four different conditions were examined to explore the effects of formic acid and iodide on WSOC: with neither formic acid nor KI (condition I), with formic acid (condition II), with KI (condition III), and with both formic acid and KI (condition IV). These four conditions maintain the same dilution ratio but with variable reagents added.

## RESULTS AND DISCUSSION

**Detection of Organic Peroxides.** The LC-ESI-MS method separated and detected the two synthesized  $\alpha$ AAHP species. Base peak intensity (BPI) chromatograms of an aqueous solution containing both  $\alpha$ AAHPs are shown in Figure 2.

LC-ESI<sup>−</sup>-MS detected  $\alpha$ AAHP-A as its deprotonated form ( $[M - H]^-$ ) due to the additional carboxylic acid functional group in the molecule (Figure 2a). Without a carboxylic acid functional group,  $\alpha$ AAHP-P is not detected as the deprotonated form. Instead, a peak with a nominal mass of 183 Da appears at the retention time ( $t_R$ ) corresponding to  $\alpha$ AAHP-P, and its elemental composition is identical to that of the deprotonated pinonic acid ( $C_{10}H_{15}O_3$ ). We propose that this peak is not pinonic acid, but instead a fragment of  $\alpha$ AAHP-P because the  $t_R$



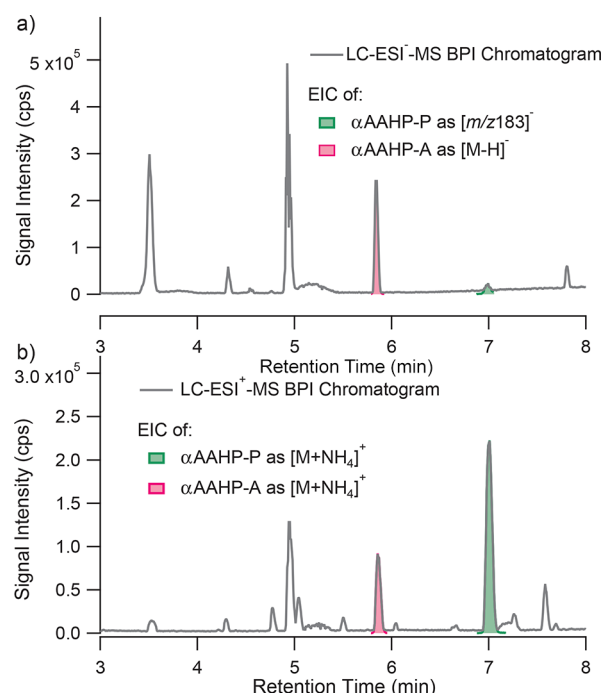


**Figure 2.** Base peak intensity (BPI) chromatogram of an aqueous solution containing  $\alpha$ AAHP-P and  $\alpha$ AAHP-A detected by (a) LC-ESI<sup>−</sup>-MS and (b) LC-ESI<sup>+</sup>-MS. Colored areas represent the extracted ion chromatograms (EICs) of these two  $\alpha$ AAHP species.

of pinonic acid is 4.7 min. In addition, as we will discuss next, this  $m/z$  183 fragment disappears when iodometry is applied, while pinonic acid does not. This observation gives rise to an important implication for the detection of SOA components, as a fraction of organic acids commonly observed by LC-ESI<sup>−</sup>-MS may have been fragments of  $\alpha$ AAHP or other high-molecular weight compounds. LC-ESI<sup>+</sup>-MS has detected the  $\alpha$ AAHP species predominantly as their ammonium clusters ( $[M + NH_4]^+$ ) but also as their sodium clusters ( $[M + Na]^+$ ). Note that the BPI chromatogram presents only the most intensive peak at each  $t_R$ .

To provide general guidance for future applications of ESI-MS in organic peroxide detection, we have also carefully evaluated the detection of organic peroxides using direct-infusion ESI-MS, which bypasses the LC component and directly injects the sample solution into the ESI-MS instrument (section S2 of the Supporting Information). Two commercially available organic peroxides, benzoyl peroxide and lauryl peroxide, were chosen as representatives for ROOR species, while the synthesized  $\alpha$ AAHP species were employed as those for multifunctional ROOH species. As expected,  $\alpha$ AAHP-P is not detected by ESI<sup>−</sup>-MS as it does not contain any carboxylic functional group. ESI<sup>−</sup>-MS detects  $\alpha$ AAHP-A as its  $[M - H]^-$  and  $[2M - H]^-$  forms. ESI<sup>−</sup>-MS detects all the four organic peroxides as their sodium clusters, as opposed to LC-ESI<sup>−</sup>-MS, in which ammonium clusters dominate. As sodium formate is introduced into the infusion system regularly for calibration, there can be a potential source of  $Na^+$  in the system. On the other hand, the amount of  $Na^+$  co-eluting with analytes during LC-ESI-MS is likely much smaller. Our results show that the difference in the ionization environment can likely change the mode of detection of organic peroxides. In future studies, the detectability of organic peroxides should be examined before any assumptions are made about their detection.

### Characterization of Iodometry and the Total Peroxide Contents of $\alpha$ -Pinene SOA.

Prior to application of iodometry to LC-ESI-MS, spectroscopy-based iodometry was performed to determine the total organic peroxide content of the WSOC samples. We performed measurements for five replicate filters. The  $H_2O_2$  equivalent concentration of total organic peroxide ranged from 14 to 30  $\mu M$ . Because the amount of SOA collected on each filter and the extraction efficiency vary, the measured total peroxide concentration of each filter extract was normalized to the measured TOC concentration.

The total peroxide content is commonly reported as molar yield (moles of organic peroxide per SOA mass) and mass yield (mass of organic peroxide per mass of SOA). Obtaining these values requires the average organic matter to organic carbon ratio (OM/OC) of SOA components and the average molecular weight of organic peroxides. Here, we assume the average OM/OC to be equivalent to that of pinic acid (i.e., 1.7), which is one of the most abundant compounds in  $\alpha$ -pinene SOA,<sup>7</sup> while the average molecular weight of 300  $g\ mol^{-1}$  for organic peroxides was adapted from previous studies.<sup>8,52</sup> With these assumptions, an average molar yield of  $(4.8 \pm 1.2) \times 10^{-10}\ mol\ \mu g^{-1}$  and an average mass yield of  $15 \pm 3.7\%$  were obtained from this study. As discussed with details in section S3.1 of the Supporting Information, this mass yield is lower but comparable to those reported in the literature.<sup>8,11,51–55</sup>

To improve our understanding of the current iodometry method, we have investigated the reaction kinetics of the iodometry reaction by monitoring the solution absorbance at 350 nm. We performed this experiment on WSOC as well as a number of individual peroxide solutions, including  $H_2O_2$ , *tert*-butyl hydroperoxide, and methyl hydroperoxide. The detailed results are presented in section S3.2 of the Supporting Information and Figure S3. Our results show that iodometry proceeds with different organic peroxides at different rates, with  $H_2O_2$  reacting with iodide the most rapidly. The reaction with WSOC may not have reached completion after 1 h, at which point the UV measurement was taken in the current and a number of past studies,<sup>8,10</sup> giving rise to a potential underestimation of the total organic peroxide content (see section S.2 of the Supporting Information).

**Iodometry-Assisted LC-ESI-MS.** Iodometry Performed on Non-Peroxide Species. Iodometry was first performed on an aqueous solution containing each of three nonperoxide organic acids at 5  $\mu M$ : adipic acid, pinonic acid, and pinic acid. These three organic acids can be readily detected by LC-ESI<sup>−</sup>-MS. An aliquot treated with iodometry (condition IV described in the Experimental Section) was compared with a control (condition II), and the BPI chromatograms are shown in section S4 of the Supporting Information. The peak intensities of the three organic acids treated with and without iodometry are essentially identical, confirming that iodide does not react with non-peroxide compounds. Another important observation is that the  $t_R$  of the three organic acids is not affected by iodometry. For the iodometry-treated sample, a large peak of iodide (127 Da) emerges at the beginning of the chromatogram ( $t_R < 2\ min$ ) but is directed to waste.

**Iodometry Performed on  $\alpha$ AAHP Species.** Iodometry was performed on an acetonitrile solution containing both of the synthesized  $\alpha$ AAHP species. Acetonitrile is used here to minimize hydrolysis of  $\alpha$ AAHPs and to ensure that the spectral changes are induced by only iodometry. The solution was

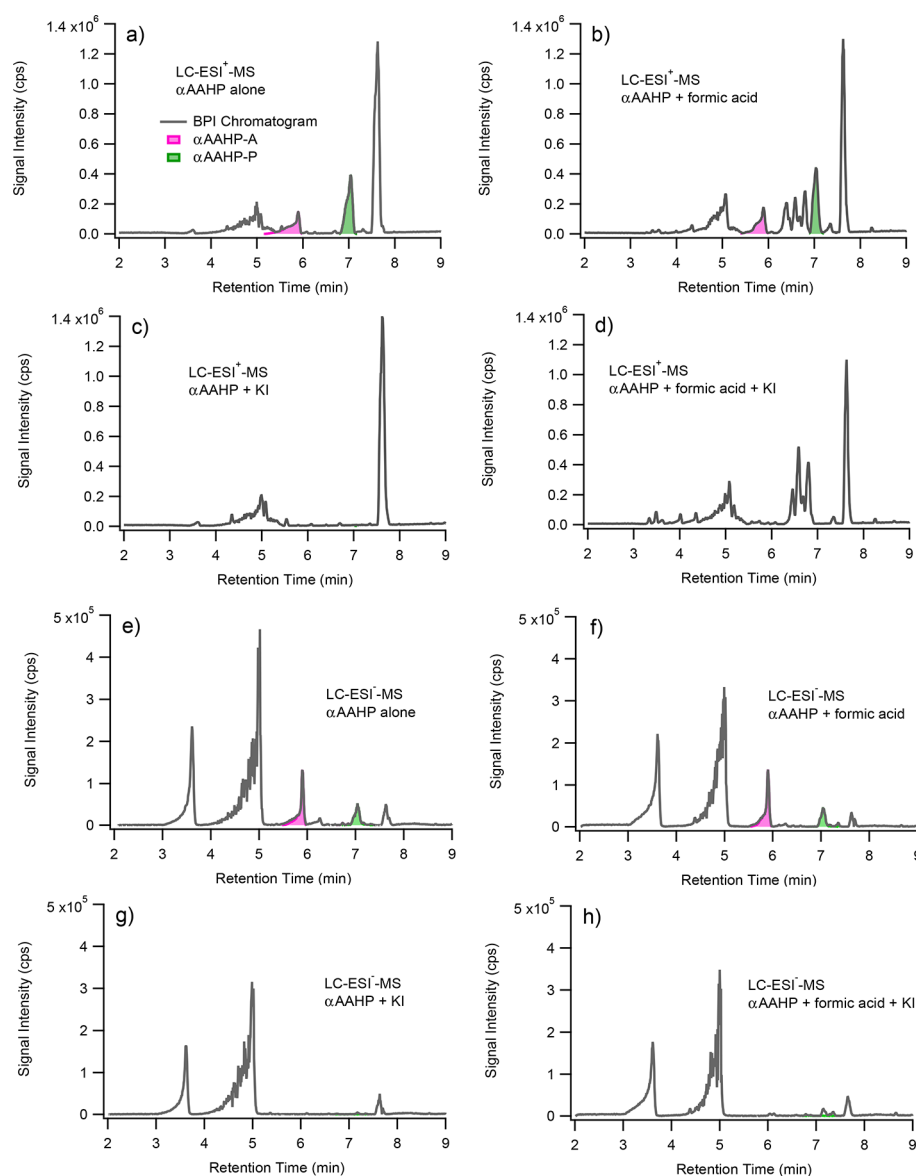


**Figure 3.** Results of iodometry performed on a mixture of synthesized  $\alpha$ AAHP-P and  $\alpha$ AAHP-A dissolved in acetonitrile. Results of LC-ESI<sup>+</sup>-MS and LC-ESI<sup>-</sup>-MS are presented in panels (a–d) and (e–h), respectively.

allowed to react for 2 h before LC-ESI-MS measurement. To the best of our knowledge, this is the first investigation of the iodometry reaction at the molecular level; therefore, detailed results are presented in Figure 3. Panels (a–d) of Figure 3 show the results obtained with LC-ESI<sup>+</sup>-MS. When formic acid was added to the solution, several additional peaks appeared on the chromatogram, but the  $\alpha$ AAHP peaks were unaffected (Figure 3b). When KI was added to the solution, either with or without formic acid, only the  $\alpha$ AAHP peaks disappeared (Figure 3c,d). The excess of organic acid added to the solution for the synthesis likely made the solution sufficiently acidic, and iodometry proceeds without additional formic acid. A similar observation was obtained using LC-ESI<sup>-</sup>-MS (Figure 3e–h). In particular, the  $m/z$  183 peak at a  $t_R$  of 7 min disappears with iodometry, confirming that it is likely a fragment of  $\alpha$ AAHP-P and unrelated to pinonic acid. These results illustrate that iodometry selectively reacts away organic peroxides with a negligible impact on non-peroxide species.

**Effect of Iodometry on the SOA Extract. Negative Mode (LC-ESI<sup>-</sup>-MS).** Analysis of  $\alpha$ -pinene SOA components using LC-ESI<sup>-</sup>-MS has been reported in a number of studies, including our previous work.<sup>17,18,20,22,26–28,56</sup> The chromatogram and mass spectra recorded in this work are provided in section S5 of the Supporting Information. The BPI chromatogram obtained in this study (Figure S5a) reproduces well those of our previous study, confirming the reproducibility of the LC-ESI-MS method. Figure S5b shows the reconstructed mass spectrum, defined to be the sum of all mass spectra at  $t_R$  values from 2 to 9 min with a peak height of  $\geq 2 \times 10^3$  counts per second (cps). The mass spectrum demonstrates a bimodal form, attributed to monomers and dimers in WSOC.<sup>28,57,58</sup> In Table S2, we provide a list of major peaks detected in this work. We did not conduct a detailed structural analysis, as this has already been done in a number of other studies.<sup>17,23,35,59</sup> Instead, we have annotated peaks that have been previously proposed as candidates of organic peroxides.

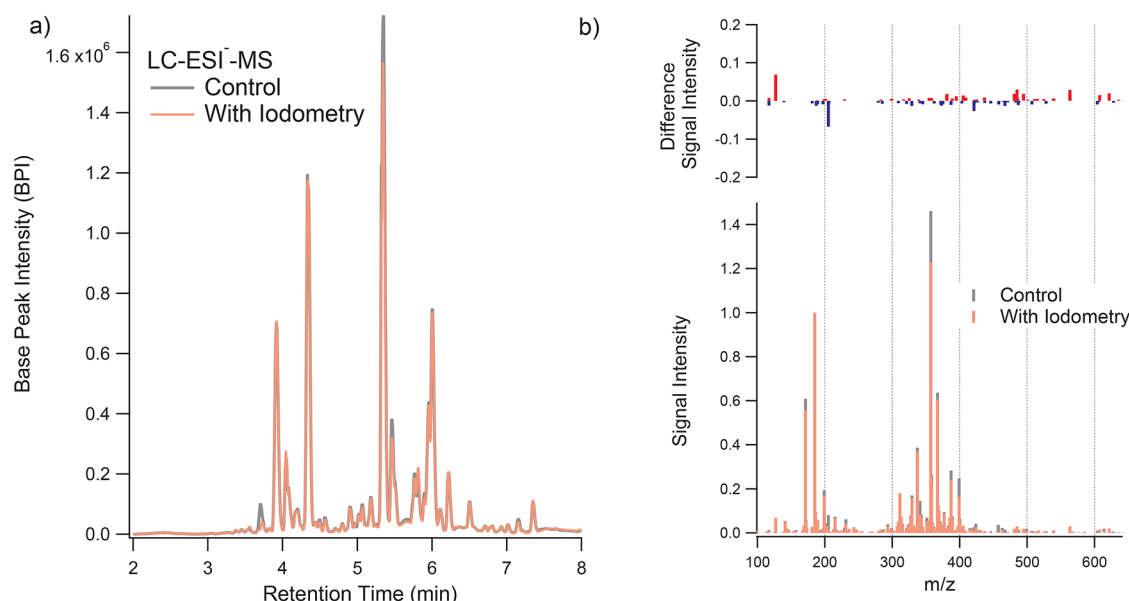


**Figure 4.** Comparison of a sample treated with and without iodometry, measured by LC-ESI<sup>−</sup>-MS. Comparison of the base peak intensity (BPI) chromatograms is shown in panel (a). The reconstructed mass spectra are shown in the bottom part of panel (b), where the peak intensities have been normalized to that of pinic acid ( $[\text{C}_9\text{H}_{14}\text{O}_4 - \text{H}]^-$  at 185.08 Da). The top part of panel (b) shows a difference mass spectrum showing peaks that are depleted by >70% and those newly introduced by iodometry. Each BPI chromatogram and mass spectrum shown here is the average of triplicate measurements. The control sample refers to condition II described in the [Experimental Section](#), while the iodometry sample refers to condition IV.

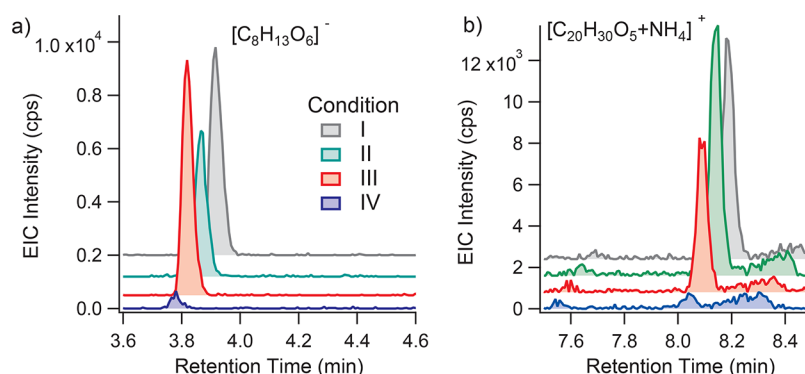


**Figure 5.** Extracted ion chromatogram (EIC) of two organic peroxide candidates: (a)  $[\text{C}_8\text{H}_{13}\text{O}_6]^-$  from LC-ESI<sup>−</sup>-MS and (b)  $[\text{C}_{20}\text{H}_{30}\text{O}_5 + \text{NH}_4]^+$  from LC-ESI<sup>+</sup>-MS. From top to bottom, the four traces represent iodometry conditions I–IV, respectively (see the [Experimental Section](#)).

We performed a comparison of samples treated with and without iodometry, and the results for LC-ESI<sup>−</sup>-MS are shown in [Figure 4](#), focusing on the comparison between the sample treated with only formic acid (condition II) and that treated with both formic acid and KI (condition IV), as this comparison excludes any mass spectral changes induced by formic acid alone and best reflects changes induced by iodometry.

Iodometry did not induce significant changes in the BPI chromatograms or reconstructed mass spectra. The top panel of [Figure 4b](#) shows the difference mass spectrum between the control and iodometry samples. Given that the reactivity of  $\alpha$ AAHP species has been exhibited ([Figure 3](#)), any organic peroxides present in the WSOC of  $\alpha$ -pinene SOA should be depleted by the time of measurement. Therefore, only peaks that exhibit a significant change, i.e., either depleted by >70% or newly introduced by iodometry, are shown in the difference mass spectrum.

The only major peak that is depleted by iodometry and showed consistency between different filter samples is that of the deprotonated form of  $\text{C}_8\text{H}_{14}\text{O}_6$  (205.071 Da,  $t_R$  of 3.71 min). The effect of iodometry on other major peaks is discussed in [section S5 of the Supporting Information](#). The decay of  $\text{C}_8\text{H}_{14}\text{O}_6$  on the BPI chromatogram can be observed ([Figure 4a](#)). The EICs of this compound are presented in [Figure 5a](#), showing that  $\text{C}_8\text{H}_{14}\text{O}_6$  is depleted only when both formic acid and KI are present. As the WSOC does not contain an excess of organic acids, compared to the synthesized  $\alpha$ AAHPs in which an organic acid is added in excess for synthesis, it seems that additional formic acid is necessary for the iodometry reaction to proceed. We have attempted to perform MS<sup>2</sup> measurements on  $\text{C}_8\text{H}_{14}\text{O}_6$ , but the signal intensities of its fragments were too low to obtain structural information.  $\text{C}_8\text{H}_{14}\text{O}_6$  has been observed previously and has been tentatively defined as an unknown carboxylic acid.<sup>17</sup> Results from this study suggest that this compound contains a peroxide functional group. Given the high oxygen/carbon ratio

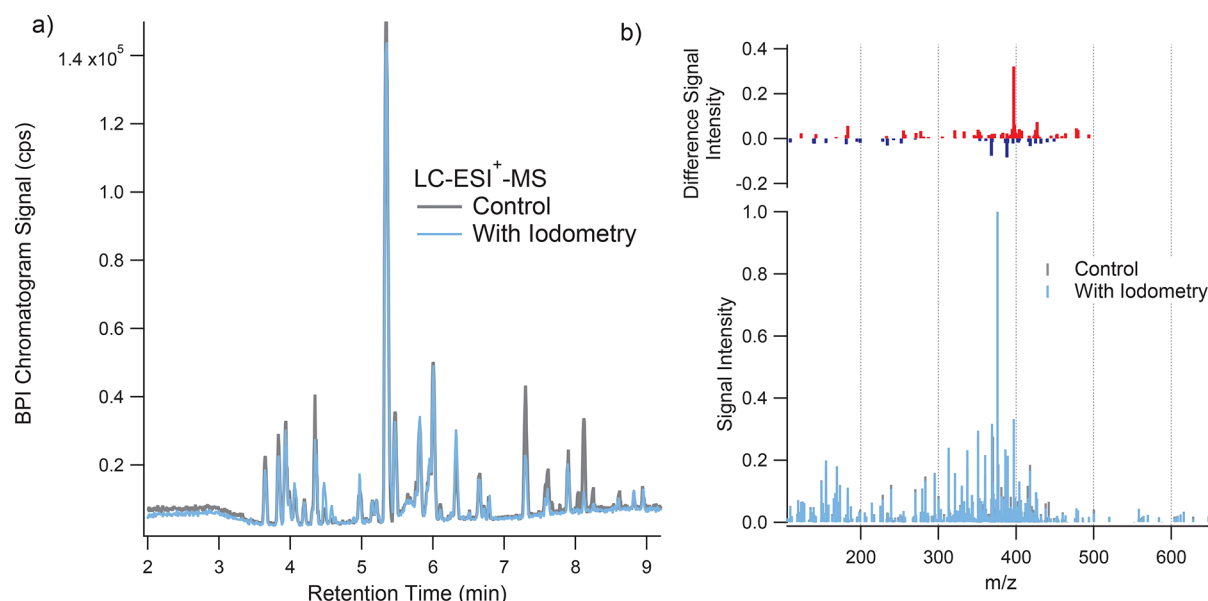


**Figure 6.** Comparison of a sample treated with and without iodometry, measured by LC-ESI<sup>+</sup>-MS. Comparison of the base peak intensity (BPI) chromatograms is shown in panel (a). The reconstructed mass spectra are shown in the bottom part of panel (b), where the peak intensities have been normalized to that of pinyldiaterpenyl ester ([C<sub>17</sub>H<sub>26</sub>O<sub>8</sub> + Na]<sup>+</sup> at 376.20 Da). The top part of panel (b) is a difference mass spectrum showing peaks that are depleted by >70% and those newly introduced by iodometry. Each BPI chromatogram and mass spectrum shown here is the average of triplicate measurements. The control sample refers to condition II described in the [Experimental Section](#), while the iodometry sample refers to condition IV.

(O/C) of this compound, C<sub>8</sub>H<sub>14</sub>O<sub>6</sub> can potentially be a HOM species arising from intramolecular hydrogen abstraction (see [Introduction](#)). Alternatively, it can also be a compound similar to 3-methyl-1,2,3-butanetricarboxylic acid (MBTCA, C<sub>8</sub>H<sub>12</sub>O<sub>6</sub>;  $t_R = 3.73$  min), a well-established organic tracer for  $\alpha$ -pinene SOA.<sup>60–62</sup>

**Positive Mode (LC-ESI<sup>+</sup>-MS).** Driven by the abundance of organic acids, the use of ESI<sup>+</sup> has prevailed in molecular analyses of  $\alpha$ -pinene SOA components. Only a few studies have employed ESI<sup>+</sup>.<sup>24,35,37,56,59,63</sup> The BPI chromatogram recorded by LC-ESI<sup>+</sup>-MS and its reconstructed mass spectrum are shown in panels (a) and (c) of [Figure S5](#), respectively. A number of major compounds are detected in positive and negative modes, while some can be detected only by the positive mode, as clusters of H<sup>+</sup>, Na<sup>+</sup>, and NH<sub>4</sub><sup>+</sup>. Because the polarity of ESI detection does not affect the chromatographic  $t_R$ , we have made peak assignments for the positive mode by comparison with peaks detected in the negative mode, and major compounds are listed in [Table S3](#).

Comparison of a sample treated with and without iodometry is shown in [Figure 6](#) in the same manner as in [Figure 4](#). The only noticeable change on the BPI chromatograms is that two major peaks, appearing at  $t_R$  values of 7.3 and 8.1 min, disappear when iodometry is applied. Judging solely on the basis of the comparison of conditions II and IV, which is the case for [Figure 6](#), these two peaks appear to be organic peroxides. However, a detailed investigation of these peaks under all four conditions, presented in [section S6.1 of the Supporting Information](#), indicates that the addition of formic acid has introduced artifacts, and these two peaks are unlikely to be peroxides. Among all the peaks with a peak height of  $\geq 2000$  cps, five appear to be candidates for organic peroxides: [C<sub>8</sub>H<sub>10</sub>O<sub>3</sub> + H]<sup>+</sup> (155.07 Da), [C<sub>10</sub>H<sub>16</sub>O<sub>5</sub> + NH<sub>4</sub>]<sup>+</sup> (234.13.34 Da), [C<sub>10</sub>H<sub>18</sub>O<sub>6</sub> + NH<sub>4</sub>]<sup>+</sup> (252.15 Da), [C<sub>20</sub>H<sub>30</sub>O<sub>5</sub> + NH<sub>4</sub>]<sup>+</sup> (368.24 Da), and [C<sub>19</sub>H<sub>30</sub>O<sub>7</sub> + NH<sub>4</sub>]<sup>+</sup> (388.23 Da). The EICs

of [C<sub>20</sub>H<sub>30</sub>O<sub>5</sub> + NH<sub>4</sub>]<sup>+</sup> under condition I–IV are shown in [Figure S5b](#), while those of the others are presented in [section S6.2 of the Supporting Information](#). [C<sub>8</sub>H<sub>10</sub>O<sub>3</sub> + H]<sup>+</sup> and [C<sub>10</sub>H<sub>16</sub>O<sub>5</sub> + NH<sub>4</sub>]<sup>+</sup> are detected as multiple peaks, and not all of them appear to be organic peroxides. This observation demonstrates the ability of iodometry-assisted LC-ESI-MS to resolve organic peroxides from non-peroxide isomers. The consistency of these observed trends has been confirmed with a separate filter sample. All five candidates for organic peroxides are detected as minor peaks and do not belong to the group of the 50 largest peaks summarized in [Table S3](#). Their peak areas are 2–5% of that of pinyldiaterpenyl ester, which is the largest peak detected by LC-ESI<sup>+</sup>-MS. The effect of iodometry on other major peaks is presented in [section S5 of the Supporting Information](#).

**Explanations for the Absence of Organic Peroxides in WSOC.** The absence of organic peroxides among the major products was unexpected, as  $\alpha$ -pinene SOA has been believed to contain a high organic peroxide content.<sup>9,64</sup> In fact, our conventional iodometry measurement using UV–vis detected a total organic peroxide content comparable to that found in previous studies ([Table S1](#)). Many of the proposed organic peroxides from previous studies<sup>17,18,23,59</sup> are detected in this work with the corresponding elemental compositions ([Table S2](#)). However, none of these compounds decayed in response to the iodometry treatment. We have altered a number of experimental and instrumental conditions that can potentially affect iodometry and the detection of organic peroxides, including the temperature of the iodometry reaction and the ESI settings. Detailed results of these experiments are presented in [section S7 of the Supporting Information](#). However, varying these factors did not explain the absence of major organic peroxide peaks.

The current LC-ESI-MS method is not quantitative, as determination of electrospray ionization efficiency for com-



pounds without definite structural information is difficult; therefore, the peak area of a compound does not directly reflect its concentration in the WSOC sample. With a computational approach, our previous study<sup>23</sup> has found that the ionization efficiencies of the dimer esters are 3–10 times higher than those of the monomeric compounds. Currently, we cannot rule out the possibility that LC-ESI-MS fails to detect certain organic peroxide species due to inefficient ionization. In particular, the major peaks detected by the current method include very few HOM compounds that typically exhibit O/C ratios of >0.7. It is likely that our method and/or instrument is less optimized toward HOMs than those of a number of previous studies.<sup>34,35,37</sup>

Alternatively, decomposition of organic peroxides may play an important role in filter extraction-based techniques. Decomposition can occur at different stages of the experiment. Highly labile organic peroxides may decompose in suspended particles before they can be collected.<sup>12,15,23,52</sup> Decomposition may also occur on the filter, with longer collection times leading to a loss of organic peroxide.<sup>52</sup> In future applications, the filter collection duration can be shortened from that in the current work (15–18 h) to minimize decomposition and evaporation. Finally, decomposition may occur after the SOA component is extracted to condensed phases, forming the OH radical<sup>16</sup> and H<sub>2</sub>O<sub>2</sub>.<sup>53,55,65</sup> Small and polar peroxides, such as H<sub>2</sub>O<sub>2</sub>, can contribute to the total peroxide content measured by the conventional, spectroscopy-based iodometry but cannot be detected by our LC-ESI-MS method, which is optimized for monomeric and dimeric oxidation products of  $\alpha$ -pinene.

## ENVIRONMENTAL IMPLICATIONS

With an emerging awareness of the role that organic peroxides play in SOA formation and the consequent health effects, identification of particle-phase organic peroxides has become a priority in atmospheric chemistry research. Employing advanced MS techniques, many recent studies have reported detection of particle-phase organic peroxides. However, structural assignment with MS is often based only on exact mass and/or fragmentation patterns, supported by feasible formation mechanisms, leaving room for potential misassignment due to a lack of structural information about functional groups. In this work, we have developed a novel technique, iodometry-assisted LC-ESI-MS, to unambiguously identify organic peroxides present in extracted SOA components at the molecular level.

Because of a lack of commercially available organic peroxides, characterization of our method was performed with synthesized  $\alpha$ -acyloxyalkyl hydroperoxides ( $\alpha$ AAHPs). Detection of  $\alpha$ AAHPs was successful, but our results reveal concerns regarding the use of ESI-MS for the detection of organic peroxides. In particular, even with the same ESI-MS instrument, a difference in the ionization mode was observed between direct infusion and LC-ESI-MS, likely due to different ionization conditions. In future studies, the utility of LC-ESI-MS for organic peroxide identification should be thoroughly characterized.

The utility of iodometry-assisted LC-ESI-MS has been demonstrated with  $\alpha$ AAHPs. Iodometry selectively reacts away organic peroxides with negligible interference with non-peroxide species. While iodometry-assisted LC-ESI-MS was applied in this work to study one specific issue related to atmospheric particulate matter, the versatility of this technique makes it applicable to a wide range of environmental

applications that require the determination of organic peroxides at the molecular level.

Iodometry-assisted LC-ESI-MS was applied to the water-soluble organic carbon (WSOC) of  $\alpha$ -pinene SOA collected from a flow tube reactor, following a standard sample collection procedure. Unexpectedly, only a limited number of detectable compounds, C<sub>8</sub>H<sub>14</sub>O<sub>6</sub> from the negative mode and five minor peaks from the positive mode, appeared to be organic peroxides. This observation is inconsistent with conventional, spectroscopy-based iodometry, which suggests that the average mass yield of organic peroxides is 15% in this system. We propose that the multifunctional organic peroxides may have decomposed to smaller peroxides that cannot be detected with the current LC-ESI-MS technique. Future studies should investigate the stability and decomposition mechanisms of organic peroxides on filters and in extraction solutions. Although this work focused only on the decay of organic peroxides during iodometry, an interesting direction would be the investigation of the corresponding alcohols arising from iodometry. Unlike organic peroxides, functionalized alcohols and polyols are commercially available, which may lead to new avenues for quantifying organic peroxides.

Our results raise significant concerns about all filter extraction-based studies of atmospheric SOA, showing that labile organic peroxides can be lost either during sample collection or after extraction. The use of MS prevails in the field of atmospheric chemistry, and the versatility of LC-ESI-MS has been proven by many studies. However, previously unrecognized considerations are required for the interpretation of MS data, particularly for the assignment of organic peroxides.

## ASSOCIATED CONTENT

### Supporting Information

The Supporting Information is available free of charge on the ACS Publications website at DOI: 10.1021/acs.est.7b04863.

Additional information about the generation and collection of SOA (section S1), detection of organic peroxides with direct-infusion ESI-MS (section S2), a comparison of the total organic peroxide content obtained in this work to those from previous studies and a detailed characterization of the iodometry method (section S3), results from iodometry performed on non-peroxide species (section S4), chromatograms and lists of major compounds detected by LC-ESI-MS (section S5), additional information about the analyses of iodometry-assisted LC-ESI-MS (section S6), and additional examination of various instrumental conditions for iodometry-assisted LC-ESI-MS (section S7) (PDF)

## AUTHOR INFORMATION

### Corresponding Author

\*E-mail: rzhao@caltech.edu. Phone: +1 626-395-8928.

### ORCID

Ran Zhao: 0000-0002-1096-7632

Christopher M. Kenseth: 0000-0003-3188-2336

John H. Seinfeld: 0000-0003-1344-4068

### Notes

The authors declare no competing financial interest.



## ACKNOWLEDGMENTS

The authors thank Dwight and Christine Landis for their generous contribution to the CPOT, Prof. Paul Wennberg for helpful discussion, Dr. John Crounse for assistance with UV-vis measurements, and Dr. Michelle Kim for the synthesis of methylhydroperoxide. LC-ESI-MS and TOC analyses were performed in the Environmental Analysis Center (EAC). This work was supported by National Science Foundation Grants AGS-1523500 and CHE-1508526. R.Z. also acknowledges support from a Natural Science and Engineering Research Council of Canada Postdoctoral Fellowship (NSERC-PDF).

## REFERENCES

- (1) Sakugawa, H.; Kaplan, I. R.; Tsai, W.; Cohen, Y. Atmospheric hydrogen peroxide. *Environ. Sci. Technol.* **1990**, *24*, 1452–1462.
- (2) Pandis, S. N.; Seinfeld, J. H. Sensitivity analysis of a chemical mechanism for aqueous-phase atmospheric chemistry. *J. Geophys. Res.* **1989**, *94*, 1105–1126.
- (3) Tao, F.; Gonzalez-Flecha, B.; Kobzik, L. Reactive oxygen species in pulmonary inflammation by ambient particulates. *Free Radical Biol. Med.* **2003**, *35*, 327–340.
- (4) Seinfeld, J. H.; Pandis, S. N. *Atmospheric Chemistry and Physics: From Air Pollution to Climate Change*, 3rd ed.; John Wiley & Sons: Hoboken, NJ, 2016.
- (5) Pye, H. O. T.; Chan, A. W. H.; Barkley, M. P.; Seinfeld, J. H. Global modeling of organic aerosol: the importance of reactive nitrogen ( $\text{NO}_x$  and  $\text{NO}_3$ ). *Atmos. Chem. Phys.* **2010**, *10*, 11261–11276.
- (6) Spracklen, D. V.; Jimenez, J. L.; Carslaw, K. S.; Worsnop, D. R.; Evans, M. J.; Mann, G. W.; Zhang, Q.; Canagaratna, M. R.; Allan, J.; Coe, H.; McFiggans, G.; Rap, A.; Forster, P. Aerosol mass spectrometer constraint on the global secondary organic aerosol budget. *Atmos. Chem. Phys.* **2011**, *11*, 12109–12136.
- (7) Kanakidou, M.; et al. Organic aerosol and global climate modelling: a review. *Atmos. Chem. Phys.* **2005**, *5*, 1053–1123.
- (8) Docherty, K. S.; Wu, W.; Lim, Y. B.; Ziemann, P. J. Contributions of organic peroxides to secondary aerosol formed from reactions of monoterpenes with  $\text{O}_3$ . *Environ. Sci. Technol.* **2005**, *39*, 4049–4059.
- (9) Bonn, B.; von Kuhlmann, R.; Lawrence, M. G. High contribution of biogenic hydroperoxides to secondary organic aerosol formation. *Geophys. Res. Lett.* **2004**, *31*, L10108.
- (10) Mutzel, A.; Rodigast, M.; Iinuma, Y.; Böge, O.; Herrmann, H. An improved method for the quantification of SOA bound peroxides. *Atmos. Environ.* **2013**, *67*, 365–369.
- (11) Mertes, P.; Pfaffenberger, L.; Dommen, J.; Kalberer, M.; Baltensperger, U. Development of a sensitive long path absorption photometer to quantify peroxides in aerosol particles (Peroxide-LOPAP). *Atmos. Meas. Tech.* **2012**, *5*, 2339–2348.
- (12) Krapf, M.; El Haddad, I.; Bruns, E. A.; Molteni, U.; Daellenbach, K. R.; Prévôt, A. S.; Baltensperger, U.; Dommen, J. Labile Peroxides in Secondary Organic Aerosol. *Chem.* **2016**, *1*, 603–616.
- (13) Bloomfield, M. The spectrophotometric determination of hydroperoxide and peroxide in a lipid pharmaceutical product by flow injection analysis. *Analyst* **1999**, *124*, 1865–1871.
- (14) Banerjee, D. K.; Budke, C. C. Spectrophotometric determination of traces of peroxides in organic solvents. *Anal. Chem.* **1964**, *36*, 792–796.
- (15) Riva, M.; Budisulistiorini, S. H.; Zhang, Z.; Gold, A.; Thornton, J. A.; Turpin, B. J.; Surratt, J. D. Multiphase reactivity of gaseous hydroperoxide oligomers produced from isoprene ozonolysis in the presence of acidified aerosols. *Atmos. Environ.* **2017**, *152*, 314–322.
- (16) Tong, H.; Arangio, A. M.; Lakey, P. S. J.; Berkemeier, T.; Liu, F.; Kampf, C. J.; Brune, W. H.; Pöschl, U.; Shiraiwa, M. Hydroxyl radicals from secondary organic aerosol decomposition in water. *Atmos. Chem. Phys.* **2016**, *16*, 1761–1771.
- (17) Kristensen, K.; Watne, a. K.; Hammes, J.; Lutz, A.; Petäjä, T.; Hallquist, M.; Bilde, M.; Glasius, M. High-molecular weight dimer esters are major products in aerosols from  $\alpha$ -pinene ozonolysis and the boreal forest. *Environ. Sci. Technol. Lett.* **2016**, *3*, 280–285.
- (18) Kristensen, K.; Cui, T.; Zhang, H.; Gold, A.; Glasius, M.; Surratt, J. D. Dimers in  $\alpha$ -pinene secondary organic aerosol: effect of hydroxyl radical, ozone, relative humidity and aerosol acidity. *Atmos. Chem. Phys.* **2014**, *14*, 4201–4218.
- (19) Kristensen, K.; Enggrob, K. L.; King, S. M.; Worton, D. R.; Platt, S. M.; Mortensen, R.; Rosenoern, T.; Surratt, J. D.; Bilde, M.; Goldstein, A. H.; Glasius, M. Formation and occurrence of dimer esters of pinene oxidation products in atmospheric aerosols. *Atmos. Chem. Phys.* **2013**, *13*, 3763–3776.
- (20) Yasmeen, F.; Vermeylen, R.; Szmigielski, R.; Iinuma, Y.; Böge, O.; Herrmann, H.; Maenhaut, W.; Claeys, M. Terpenylic acid and related compounds: precursors for dimers in secondary organic aerosol from the ozonolysis of  $\alpha$ - and  $\beta$ -pinene. *Atmos. Chem. Phys.* **2010**, *10*, 9383–9392.
- (21) Yasmeen, F.; Vermeylen, R.; Maurin, N.; Perraudin, E.; Doussin, J.-F.; Claeys, M. Characterisation of tracers for aging of  $\alpha$ -pinene secondary organic aerosol using liquid chromatography/negative ion electrospray ionisation mass spectrometry. *Environ. Chem.* **2012**, *9*, 236–246.
- (22) Zhang, X.; Dalleska, N. F.; Huang, D. D.; Bates, K. H.; Sorooshian, A.; Flagan, R. C.; Seinfeld, J. H. Time-resolved molecular characterization of organic aerosols by PILS+ UPLC/ESI-Q-TOFMS. *Atmos. Environ.* **2016**, *130*, 180–189.
- (23) Zhang, X.; McVay, R. C.; Huang, D. D.; Dalleska, N. F.; Aumont, B.; Flagan, R. C.; Seinfeld, J. H. Formation and evolution of molecular products in  $\alpha$ -pinene secondary organic aerosol. *Proc. Natl. Acad. Sci. U. S. A.* **2015**, *112*, 14168–14173.
- (24) Witkowski, B.; Gierczak, T. Early stage composition of SOA produced by  $\alpha$ -pinene/ozone reaction:  $\alpha$ -Acloxyhydroperoxy aldehydes and acidic dimers. *Atmos. Environ.* **2014**, *95*, 59–70.
- (25) Hall, W. A., VI; Johnston, M. V. Oligomer content of  $\alpha$ -pinene secondary organic aerosol. *Aerosol Sci. Technol.* **2011**, *45*, 37–45.
- (26) Müller, L.; Reinnig, M.-C.; Warnke, J.; Hoffmann, T. Unambiguous identification of esters as oligomers in secondary organic aerosol formed from cyclohexene and cyclohexene/ $\alpha$ -pinene ozonolysis. *Atmos. Chem. Phys.* **2008**, *8*, 1423–1433.
- (27) Müller, L.; Reinnig, M.-C.; Hayen, H.; Hoffmann, T. Characterization of oligomeric compounds in secondary organic aerosol using liquid chromatography coupled to electrospray ionization Fourier transform ion cyclotron resonance mass spectrometry. *Rapid Commun. Mass Spectrom.* **2009**, *23*, 971–979.
- (28) Kourtchev, I.; Doussin, J.-F.; Giorio, C.; Mahon, B.; Wilson, E. M.; Maurin, N.; Pangui, E.; Venables, D. S.; Wenger, J. C.; Kalberer, M. Molecular composition of fresh and aged secondary organic aerosol from a mixture of biogenic volatile compounds: a high-resolution mass spectrometry study. *Atmos. Chem. Phys.* **2015**, *15*, 5683–5695.
- (29) Reinnig, M.-C.; Müller, L.; Warnke, J.; Hoffmann, T. Characterization of selected organic compound classes in secondary organic aerosol from biogenic VOCs by HPLC/MS<sup>n</sup>. *Anal. Bioanal. Chem.* **2008**, *391*, 171–182.
- (30) Mochida, M.; Katrib, Y.; Jayne, J. T.; Worsnop, D. R.; Martin, S. T. The relative importance of competing pathways for the formation of high-molecular-weight peroxides in the ozonolysis of organic aerosol particles. *Atmos. Chem. Phys.* **2006**, *6*, 4851–4866.
- (31) Enami, S.; Colussi, A. J. Efficient scavenging of Criegee intermediates on water by surface-active cis-pinonic acid. *Phys. Chem. Chem. Phys.* **2017**, *19*, 17044–17051.
- (32) Ehn, M.; Thornton, J. A.; Kleist, E.; Sipilä, M.; Junninen, H.; Pullinen, I.; Springer, M.; Rubach, F.; Tillmann, R.; Lee, B.; others.; et al. A large source of low-volatility secondary organic aerosol. *Nature* **2014**, *506*, 476–479.
- (33) Crounse, J. D.; Nielsen, L. C.; Jørgensen, S.; Kjaergaard, H. G.; Wennberg, P. O. Autoxidation of organic compounds in the atmosphere. *J. Phys. Chem. Lett.* **2013**, *4*, 3513–3520.
- (34) Mutzel, A.; Poulain, L.; Berndt, T.; Iinuma, Y.; Rodigast, M.; Böge, O.; Richters, S.; Spindler, G.; Sipilä, M.; Jokinen, T.; Kulmala, M.; Herrmann, H. Highly Oxidized Multifunctional Organic

Compounds Observed in Tropospheric Particles: A Field and Laboratory Study. *Environ. Sci. Technol.* **2015**, *49*, 7754–7761.

(35) Zhang, X.; et al. Highly oxygenated multifunctional compounds in  $\alpha$ -pinene secondary organic aerosol. *Environ. Sci. Technol.* **2017**, *51*, 5932–5940.

(36) Lee, B. H.; et al. Highly functionalized organic nitrates in the southeast United States: Contribution to secondary organic aerosol and reactive nitrogen budgets. *Proc. Natl. Acad. Sci. U. S. A.* **2016**, *113*, 1516–1521.

(37) Tu, P.; Hall, W. A.; Johnston, M. V. Characterization of highly oxidized molecules in fresh and aged biogenic secondary organic aerosol. *Anal. Chem.* **2016**, *88*, 4495–4501.

(38) Oss, M.; Krueve, A.; Herodes, K.; Leito, I. Electrospray ionization efficiency scale of organic compounds. *Anal. Chem.* **2010**, *82*, 2865–2872.

(39) Cech, N. B.; Enke, C. G. Practical implications of some recent studies in electrospray ionization fundamentals. *Mass Spectrom. Rev.* **2001**, *20*, 362–387.

(40) Steimer, S. S.; Kourtchev, I.; Kalberer, M. Mass spectrometry characterization of peroxydicarboxylic acids as proxies for reactive oxygen species and highly oxygenated molecules in atmospheric aerosols. *Anal. Chem.* **2017**, *89*, 2873–2879.

(41) Ferdousi, B. N.; Islam, M. M.; Okajima, T.; Ohsaka, T. Electrochemical, HPLC and electrospray ionization mass spectroscopic analyses of peroxydicarboxylic acid coexisting with citric acid and hydrogen peroxide in aqueous solution. *Talanta* **2008**, *74*, 1355–1362.

(42) Nilsson, J.; Carlberg, J.; Abrahamsson, P.; Hulthe, G.; Persson, B.-A.; Karlberg, A.-T. Evaluation of ionization techniques for mass spectrometric detection of contact allergenic hydroperoxides formed by autooxidation of fragrance terpenes. *Rapid Commun. Mass Spectrom.* **2008**, *22*, 3593–3598.

(43) Yin, H.; Hachey, D. L.; Porter, N. A. Structural analysis of diacyl peroxides by electrospray tandem mass spectrometry with ammonium acetate: bond homolysis of peroxide-ammonium and peroxide-proton adducts. *Rapid Commun. Mass Spectrom.* **2000**, *14*, 1248–1254.

(44) Witkowski, B.; Gierczak, T. Analysis of  $\alpha$ -acyloxyhydroperoxy aldehydes with electrospray ionization-tandem mass spectrometry (ESI-MS(n)). *J. Mass Spectrom.* **2013**, *48*, 79–88.

(45) Weber, R. J.; Orsini, D.; Daun, Y.; Lee, Y.-N.; Klotz, P. J.; Brechtel, F. A particle-into-liquid collector for rapid measurement of aerosol bulk chemical composition. *Aerosol Sci. Technol.* **2001**, *35*, 718–727.

(46) Kondo, Y.; Miyazaki, Y.; Takegawa, N.; Miyakawa, T.; Weber, R. J.; Jimenez, J. L.; Zhang, Q.; Worsnop, D. R. Oxygenated and water-soluble organic aerosols in Tokyo. *J. Geophys. Res.* **2007**, *112*, D01203 DOI: 10.1029/2006JD007056.

(47) Lee, A. K. Y.; Hayden, K. L.; Herckes, P.; Leaitch, W. R.; Liggio, J.; Macdonald, A. M.; Abbatt, J. P. D. Characterization of aerosol and cloud water at a mountain site during WACS 2010: secondary organic aerosol formation through oxidative cloud processing. *Atmos. Chem. Phys.* **2012**, *12*, 7103–7116.

(48) Herckes, P.; Valsaraj, K. T.; Collett, J. L., Jr A review of observations of organic matter in fogs and clouds: Origin, processing and fate. *Atmos. Res.* **2013**, *132–133*, 434–449.

(49) Blando, J. D.; Turpin, B. J. Secondary organic aerosol formation in cloud and fog droplets: a literature evaluation of plausibility. *Atmos. Environ.* **2000**, *34*, 1623–1632.

(50) Huang, Y.; Coggon, M. M.; Zhao, R.; Lignell, H.; Bauer, M. U.; Flagan, R. C.; Seinfeld, J. H. The Caltech Photooxidation Flow Tube reactor: design, fluid dynamics and characterization. *Atmos. Meas. Tech.* **2017**, *10*, 839–867.

(51) Epstein, S. A.; Blair, S. L.; Nizkorodov, S. A. Direct photolysis of  $\alpha$ -pinene ozonolysis secondary organic aerosol: effect on particle mass and peroxide content. *Environ. Sci. Technol.* **2014**, *48*, 11251–11258.

(52) Li, H.; Chen, Z.; Huang, L.; Huang, D. Organic peroxides' gas-particle partitioning and rapid heterogeneous decomposition on secondary organic aerosol. *Atmos. Chem. Phys.* **2016**, *16*, 1837–1848.

(53) Badali, K. M.; Zhou, S.; Aljawhary, D.; Antinölo, M.; Chen, W. J.; Lok, A.; Mungall, E.; Wong, J. P. S.; Zhao, R.; Abbatt, J. P. D.

Formation of hydroxyl radicals from photolysis of secondary organic aerosol material. *Atmos. Chem. Phys.* **2015**, *15*, 7831–7840.

(54) Chen, X.; Hopke, P. K. Secondary organic aerosol from  $\alpha$ -pinene ozonolysis in dynamic chamber system. *Indoor Air* **2009**, *19*, 335–345.

(55) Wang, Y.; Kim, H.; Paulson, S. E. Hydrogen peroxide generation from  $\alpha$ - and  $\beta$ -pinene and toluene secondary organic aerosols. *Environ. Sci. Technol.* **2011**, *45*, 3149–3156.

(56) Gao, Y.; Hall, W. H.; Johnston, M. Molecular composition of monoterpene secondary organic aerosol at low mass loading. *Environ. Sci. Technol.* **2010**, *44*, 7897–7902.

(57) Aljawhary, D.; Lee, A. K. Y.; Abbatt, J. P. D. High-resolution chemical ionization mass spectrometry (ToF-CIMS): application to study SOA composition and processing. *Atmos. Meas. Tech.* **2013**, *6*, 3211–3224.

(58) Zhao, R.; Aljawhary, D.; Lee, A. K. Y.; Abbatt, J. P. D. Rapid aqueous-phase photooxidation of dimers in the  $\alpha$ -pinene secondary organic aerosol. *Environ. Sci. Technol. Lett.* **2017**, *4*, 205–210.

(59) Venkatachari, P.; Hopke, P. K. Characterization of products formed in the reaction of ozone with  $\alpha$ -pinene: case for organic peroxides. *J. Environ. Monit.* **2008**, *10*, 966–974.

(60) Szmigielski, R.; Surratt, J. D.; Gómez-González, Y.; Van der Veken, P.; Kourtchev, I.; Vermeylen, R.; Blockhuys, F.; Jaoui, M.; Kleindienst, T. E.; Lewandowski, M.; Offenberg, J. H.; Edney, E. O.; Seinfeld, J. H.; Maenhaut, W.; Claeys, M. 3-methyl-1,2,3-butanetricarboxylic acid: An atmospheric tracer for terpene secondary organic aerosol. *Geophys. Res. Lett.* **2007**, *34*, L24811.

(61) Müller, L.; Reinnig, M.-C.; Naumann, K. H.; Saathoff, H.; Mentel, T. F.; Donahue, N. M.; Hoffmann, T. Formation of 3-methyl-1,2,3-butanetricarboxylic acid via gas phase oxidation of pinonic acid - a mass spectrometric study of SOA aging. *Atmos. Chem. Phys.* **2012**, *12*, 1483–1496.

(62) Aljawhary, D.; Zhao, R.; Lee, A. K.; Wang, C.; Abbatt, J. P. Kinetics, mechanism and secondary organic aerosol yield of aqueous phase photo-oxidation of  $\alpha$ -pinene oxidation products. *J. Phys. Chem. A* **2016**, *120*, 1395–1407.

(63) Gao, S.; Keywood, M.; Ng, N. L.; Surratt, J.; Varutbangkul, V.; Bahreini, R.; Flagan, R. C.; Seinfeld, J. H. Low-molecular-weight and oligomeric components in secondary organic aerosol from the ozonolysis of cycloalkenes and  $\alpha$ -pinene. *J. Phys. Chem. A* **2004**, *108*, 10147–10164.

(64) Jenkin, M. E. Modelling the formation and composition of secondary organic aerosol from  $\alpha$ - and  $\beta$ -pinene ozonolysis using MCM v3. *Atmos. Chem. Phys.* **2004**, *4*, 1741–1757.

(65) Arellanes, C.; Paulson, S. E.; Fine, P. M.; Sioutas, C. Exceeding of Henry's law by hydrogen peroxide associated with urban aerosols. *Environ. Sci. Technol.* **2006**, *40*, 4859–4866.